ACS OMEGA

http://pubs.acs.org/journal/acsodf

Article

Time-Dependent Density Functional Theory Investigation on the Electronic and Optical Properties of Poly-C,Si,Ge-acenes

Paola Mocci, Giuliano Malloci,* Andrea Bosin, and Giancarlo Cappellini*

Cite This: https://dx.doi.org/10.1021/acsomega.0c01516

Read Online

ACCESS | Metrics & More | Article Recommendations

ABSTRACT: We report a comparative computational investigation on the first six members of linear poly-C,Si,Ge-acenes ($X_{4n+2}H_{2n+4}$, X = C,Si,Ge; n = 1, 2, 3, 4, 5, 6). We performed density functional theory (DFT) and time-dependent DFT calculations to compare morphological, electronic, and optical properties. While C-acenes are planar, Si- and Ge-acenes assume a buckled configuration. Electronic properties show similar trends as a function of size for all families. In particular, differently from C-based compounds, in the case of both Si- and Ge-acenes, the excitation energies of the strongest low-lying electronic transition (β peaks) span the visible region of the spectrum, demonstrating their size tunability. For all families, we assessed the plasmonic character of this transition and found a linear relationship for the wavelength-dependence of the β peaks as a function of the number of rings. A similar slope of about 56 nm is observed for Si- and Ge-acenes, although the peak positions of the former are located at lower wavelengths. Outcomes of this study are compared with existing theoretical results for 2D lattices and nanoribbons, and experiments where available.

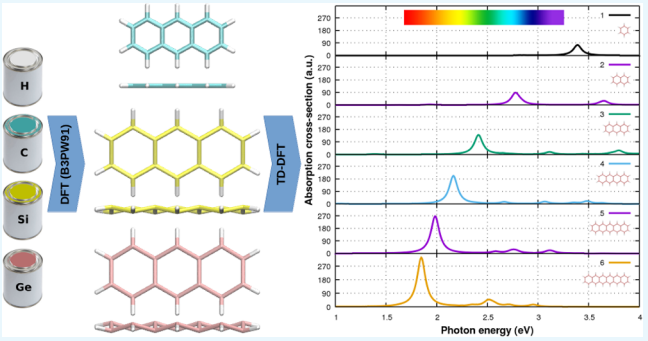

INTRODUCTION

The discovery of graphene in 2004[1] has opened the way to the synthesis of new 2D-materials. The exotic properties of graphene led shortly after to the further exploration of its silicon and germanium counterparts, respectively known as silicene and germanene.[2−4] In fact, while these IV-group elements are very similar,[5] each one is characterized by significant peculiarities.[6] Due to the presence of buckling motifs deviating from the planar 2D configuration,[7] in their infinite structural appearance, silicene and germanene appear more easily integrable with substrates than graphene.[3] In addition, these materials exhibit favorable mechanical, electronic, and optical properties,[2] making them ideal systems both for fundamental research and for promising nanoelectronic applications.[8−11]

As to finite-sized compounds, linear poly-C-acenes composed of fused benzene rings[12−15] are widely used as active elements in many optoelectronic devices, ranging from photovoltaic cells, light-emitting diodes, flexible and transparent displays, liquid crystals, and organic thin-film field-effect transitors.[16−21] Analogs of these carbon-based compounds have consequently been targeted for decades. In particular, a large number of computational studies have been performed on Si-based aromatic molecules. As an example, the simplest member hexasilabenzene Si_6H_6 was first predicted to have a planar D_{6h} benzene-like structure on the basis of semi-empirical calculations,[22] and then a chair-like D_{3d} conformation[23] according to ab initio calculations. Structural transition from non-planar to planar conformations in the $Si_{6-n}C_nH_6$ (n = 0−6) series was later investigated using higher-level coupled cluster methods, showing that deviation from planarity in hexasilabenzene is caused by the pseudo-Jahn−Teller effect.[24] Further computational investigations on poly-Si,Ge-acenes[25−27] and silicene or germanene nanoribbons have been published over the years.[28−34]

From the synthesis point of view, reactions involving generation of sila-aromatic compounds, namely silabenzene,[35] 1-silanaphthalene,[36] 2-silanaphthalen,[37] and a 9-silaanthracene derivative,[38] have been reported. More recently, an X-ray diffraction study complemented by nuclear magnetic resonance and hybrid density functional theory calculations revealed a tricyclic aromatic isomer of hexasilabenzene with a chair-like silicon frame.[39]

Given the broad interest in heavy analogs of C-based compounds, in this work, we consider the Si- and Ge-acenes analogues of the widely investigated C-based linear acenes;[12−15] in particular, we focus on the first six members $X_{4n+2}H_{2n+4}$, X =

Received: April 3, 2020
Accepted: June 3, 2020

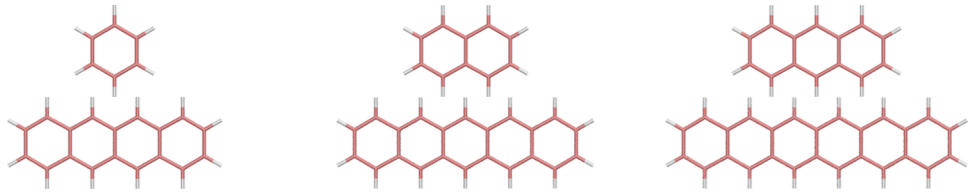

Figure 1. Top view of the poly-C,Si,Ge-acenes investigated in this work ($X_{4n+2}H_{2n+4}$; X = C,Si,Ge; n = 1, 2, 3, 4, 5, 6).

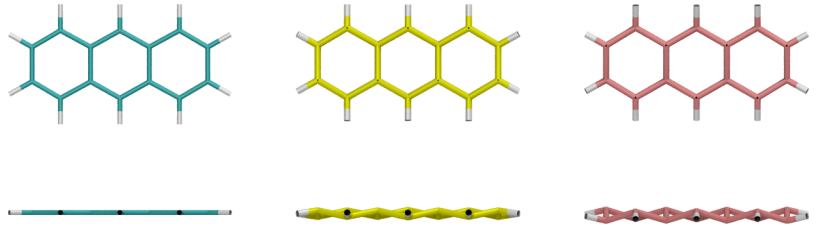

Figure 2. Top and side views of the poly-acenes $X_{14}H_{10}$, with X = C,Si,Ge from left to right, respectively.

C,Si,Ge; n = 1, 2, 3, 4, 5, 6. Morphological, electronic, and optical properties obtained via (time-dependent) density functional theory (DFT) are presented and discussed comparatively. We highlight the similarities and differences between families as well as the characteristic trends within families as a function of molecular size. We additionally compare our findings with previous theoretical results for the infinite 2D lattices and nanoribbons and with the available experimental data. A web-based repository with input and output files of our simulations is freely available at https://www.dsf.unica.it/csige.

RESULTS AND DISCUSSION

A 2D sketch of the systems under investigation is shown in Figure 1.

MORPHOLOGICAL PROPERTIES

From a morphological point of view, an inspection of the DFT-optimized geometries reveals that poly-C-acenes, as expected, maintain the planar geometry typical of the family.[12,15] On the contrary, all of the investigated poly-Si,Ge-acenes display considerable out-of-plane displacements (buckling). The qualitative comparison is shown in Figure 2 for the representative case of the 3-ring systems.

The average displacements with respect to the molecular plane are reported in Table 1 as a function of the number of rings, together with the values calculated for the 2D infinite lattice,[6,40] and for H-saturated armchair nanoribbons ASiNR-9[30] and AGeNR-9.[30,33] While the deviations registered for Si-acenes in the range n = 1−6 appear to be constant along the series, for the corresponding Ge counterparts, a slight decrease at increasing molecular size can be observed. On average, poly-Ge-acenes deviate from planarity more than poly-Si-acenes, with average deviations of about 0.307 and 0.197 Å, respectively. The above results can be compared with those obtained for the corresponding 2D infinite systems (silicene and germanene),[6] also shown in Table 1. In particular, we found that the relative deviations with respect to the corresponding 2D lattice are of the same order of magnitude, about −13% for both Si and Ge. In addition, the displacement shown by the heavier compounds is very close to the buckling amplitude calculated for H-saturated armchair nanoribbons ASiNR-9 and AGeNR-9.[30]

Figure 3 shows the buckling profile for $X_{4n+2}H_{2n+4}$, with X = Si,Ge and n = 1, 2, 3, 4, 5, 6 along the long-axis direction, i.e., the

Table 1. Average Displacements (Å) along the Out-of-Plane Direction Measured for Poly-Si,Ge-acenes and Compared with Previous Calculations for Infinite 2D Lattices and H-Saturated Nanoribbons

n	Si	Ge
This Work		
1	0.195	0.316
2	0.197	0.313
3	0.197	0.308
4	0.196	0.304
5	0.195	0.302
6	0.195	0.299
Silicene and Germanene		
2D lattice[6]	0.225	0.345
2D lattice[40]	0.225	0.340
H-Saturated Nanoribbons		
AXNR-9[30]	∼0.2	∼0.3
AGeNR-9[33]		∼0.34

absolute value of the out-of-plane displacement of Si and Ge atoms. We report only the independent displacements for each compound, the others being fixed by symmetry. Atoms are labeled from 1 to 7 according to their position, as marked on the molecule top view at the bottom; atom position 1 (leftmost) is always the outermost. Buckling is not constant, with the obvious exception of one-ring molecules, and shows very similar trends for Si and Ge. Within a single molecule, the displacement shows a kind of oscillatory behavior, which "damps" moving from outer to inner rings (for molecules with three to six rings), Si damping being faster than Ge. This is not completely unexpected given that inner rings, at least in one direction, are somehow more constrained with respect to outer ones. Note that for the latter, the profile is a flat line since the absolute out-of-plane displacements are virtually constant.

Table 2 compares our computed C−C, Si−Si, and Ge−Ge bond lengths for the smallest and largest compounds (n = 1 and n = 6) to available data for Si_6H_6,[25] 2D[6] and 3D lattices,[41] 7-ASiNR,[29] ASiNR-9, and AGeNR-9 nanoribbons.[30] Si−Si and Ge−Ge bond length profiles are additionally depicted in Figure 4 for the heaviest systems $X_{26}H_{16}$, with X = C,Si,Ge. Bonds are labeled from A to J according to their position, as marked on the molecule top view at the bottom; bonds A and G (leftmost) are always the outermost. Excluding the absolute values, the

https://dx.doi.org/10.1021/acsomega.0c01516
ACS Omega XXXX, XXX, XXX−XXX

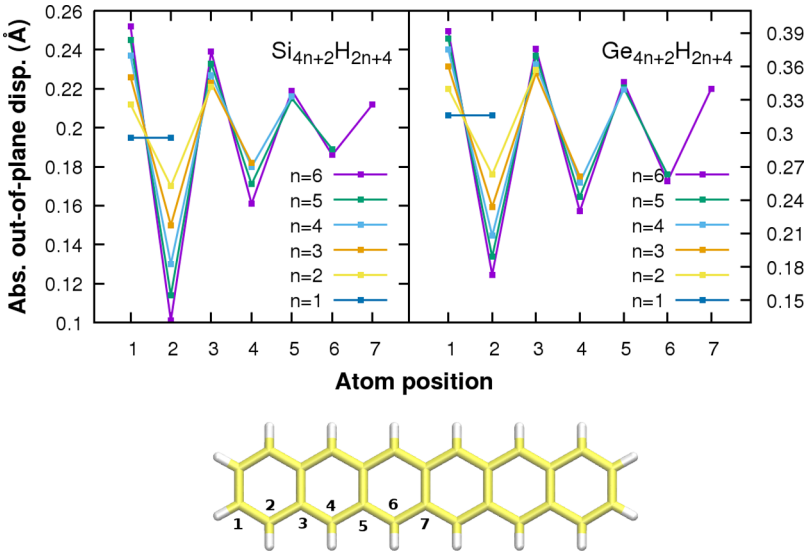

Figure 3. Profile of absolute out-of-plane displacements (buckling) for $X_{4n+2}H_{2n+4}$, with X = Si,Ge and n = 1, 2, 3, 4, 5, 6 for the atoms labeled as shown at the bottom.

Table 2. Bond Lengths (Å) for Selected Poly-C,Si,Ge-acenes

n	C	Si	Ge
This Work			
1	1.39	2.23	2.36
6 (outer ring)	1.36−1.45	2.21−2.27	2.33−2.40
6 (inner ring)	1.40−1.45	2.25−2.30	2.38−2.42
Silo-benzene			
1[25]		2.23	
2D and 3D Lattices			
2D lattice[6]	1.42	2.24	2.34
2D lattice (exp)[41]	1.54 (diamond)	2.35	2.45
H-Saturated Nanoribbons			
AXNR-9[30]		∼2.21−2.26	∼2.32−2.38
AGeNR-9[33]			∼2.4
7-ASiNR[30]		2.22−2.32	

behavior is very similar for C, Si, and Ge, and for bonds A−F shows a damped oscillation somehow similar to buckling amplitudes in Figure 3. On the contrary, bonds G to J exhibit a saturating behavior when going form outer to inner rings.

In summary, both buckling and bond profiles indicate that inner rings are more "regular" than the outer ones. Compared with the 2D lattice,[6] Si and Ge are less buckled, while Si−Si and Ge−Ge bonds are slightly longer. In addition, even if we do not have the detailed profiles for nanoribbons ASiNR-9 and AGeNR-9,[30] average values appear to be in good agreement, and the same is true for the bond length profiles of 7-ASiNR.[29]

■ ELECTRONIC PROPERTIES

The computed vertical electron affinity EA_v, vertical ionization energy IE_v, fundamental gap E_{gap} as defined by eq 1 (Computational Methods section), and HOMO−LUMO gap E_{HL} for the different systems considered are reported in Tables 3−5 and compared with previous calculations and available experimental data. The behavior of these quantities as a function of molecular size is shown in Figure 5. As expected, in all cases,

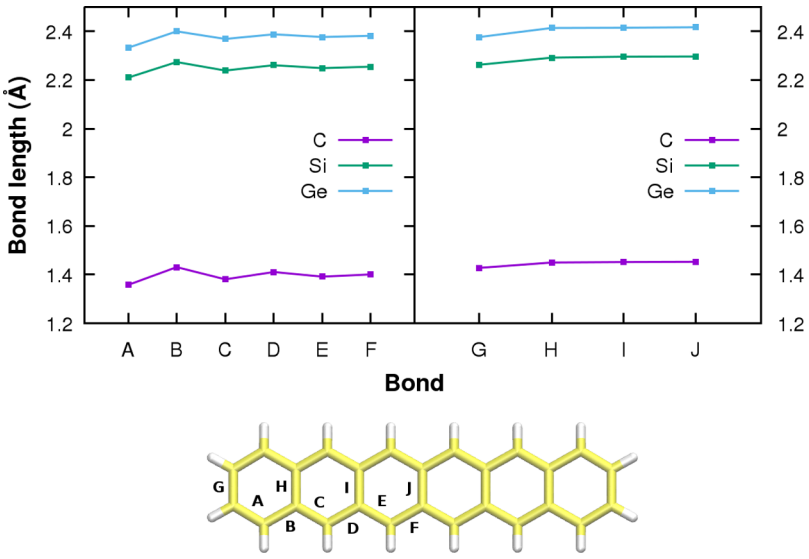

Figure 4. Profile of bond lengths for $X_{26}H_{16}$, with X = C,Si,Ge for the bonds labeled as shown at the bottom.

https://dx.doi.org/10.1021/acsomega.0c01516
ACS Omega XXXX, XXX, XXX−XXX

Table 3. Vertical Electron Affinity (EA_v), Vertical Ionization Energy (IE_v), Fundamental Gap ($E_{gap} = IE_v - EA_v$), and HOMO−LUMO Gap (E_{HL}) for the Poly-C-acenes $C_{4n+2}H_{2n+4}$, n = 1, 2, 3, 4, 5, 6[a]

n	EA_v	IE_v	E_{gap}	E_{HL}
This Work				
1	−1.64 (−1.39)	9.32 (9.20)	10.96 (10.59)	6.74 (6.60)
1 (exp)	−1.12 ± 0.03	9.24384 ± 0.00006	10.36	6.90
2	−0.39 (−0.38)	8.01 (7.89)	8.40 (8.27)	4.82 (4.74)
2 (exp)	−0.20 ± 0.05	8.144 ± 0.001	8.34	4.45
3	0.46 (0.43)	7.20 (7.09)	6.74 (6.66)	3.60 (3.54)
3 (exp)	0.530 ± 0.005	7.439 ± 0.006	6.91	3.45
4	1.04 (1.00)	6.65 (6.55)	5.61 (5.55)	2.78 (2.74)
4 (exp)	1.067 ± 0.043	6.97 ± 0.05	5.90	2.72
5	1.47 (1.41)	6.26 (6.16)	4.80 (4.75)	2.21 (2.19)
5(exp)	1.392 ± 0.043	6.589 ± 0.001	5.20	2.31
6	1.79 (1.72)	5.97 (5.87)	4.18 (4.15)	1.80 (1.78)
6 (exp)		6.36 ± 0.02		1.90
H-Saturated Nanoribbons				
−ZGNR[42]				∼0.20
−ZGNR[28]				
2D and 3D Lattices				
2D[40]	4.61	4.61	0	
2D (exp)[41]			5.4	

[a]Results from previous B3LYP/6-31 + G* calculations (between parentheses) and available experimental data as compiled in ref 12 are reported. All energies are expressed in eV.

Table 4. Vertical Electron Affinity (EA_v), Vertical Ionization Energy (IE_v), Fundamental Gap (E_{gap}), and HOMO−LUMO Gap (E_{HL}) for the Poly-Si-acenes $Si_{4n+2}H_{2n+4}$, n = 1, 2, 3, 4, 5, 6[a]

n	EA_v	IE_v	E_{gap}	E_{HL}
This Work				
1	1.22	7.42	6.20	3.22
2	2.00	6.73	4.74	2.26
3	2.50	6.32	3.81	1.68
4	2.84	6.04	3.20	1.31
5	3.08	5.85	2.76	1.06
6	3.26	5.70	2.44	0.88
H-Saturated Nanoribbons				
2-ZSiNR[29]				0.25
2D and 3D Lattices				
2D lattice[40]	4.76	4.76	0	
2D lattice + spin−orbit[40]	4.74	4.77	0.03	
2D lattice (exp)[41]			1.17	

[a]All energies are expressed in eV

Table 5. Same as Table 4 for Poly-Ge-acenes $Ge_{4n+2}H_{2n+4}$, n = 1, 2, 3, 4, 5, 6

n	EA_v	IE_v	E_{gap}	E_{HL}
This Work				
1	1.50	7.51	6.00	3.04
2	2.24	6.82	4.58	2.14
3	2.72	6.43	3.71	1.62
4	3.04	6.18	3.14	1.28
5	3.26	6.00	2.74	1.06
6	3.42	5.86	2.44	0.91
2D and 3D Lattices				
2D lattice[40]	4.46	4.46	0	
2D lattice + spin−orbit[40]	4.44	4.48	0.04	
2D lattice (exp)[41]			0.744	

the vertical ionization energy (vertical electron affinity) decreases (increases) with increasing molecular size. As shown in Table 3, the present results for poly-C-acenes are consistent with previously reported data,[12,15,43] the small differences (at most 2%) being due to the different combinations exchange-correlation functional/basis sets adopted; more importantly, the obtained results are in fair agreement with the experimental data available (compiled in refs[12,15] and reported in Table 3). Note that, in particular, while for poly-C-acenes we find negative values for the EA_v of the first two members benzene and naphthalene, in the case of poly-Si,Ge-acenes, the electron affinities are always positive.

As a consequence of the above trends, the fundamental gap E_{gap} decreases as a function of size. More specifically, the relative deviations calculated with respect to the first member of each family reveal a reduction of E_{gap} of the same order of magnitude in all cases (from −62 to −23, −61 to −23, and −59 to −24% for poly-C,Si,Ge-acenes, respectively). Note that the HOMO−LUMO gaps calculated for poly-Si-acenes $Si_{4n+2}H_{2n+4}$, n = 1, 2, 3, 4, 5 are in perfect agreement with the results of ref 8 obtained at the same level of theory.

As shown in Tables 3−5, EA and IE have been calculated for graphene, silicene, and germanene 2D lattices,[40] which are zero gap materials, so EA and IE are the same, and lie approximately midway between our EA/IE values. One could be tempted to argue that E_{gap} and E_{HL}, for large values of n tend to the values calculated for 2D lattices,[40] which show zero gap or, for Si and Ge, very small gaps if spin−orbit coupling is taken into account (see Tables 4 and 5). Unfortunately such a conclusion is not justified, due to finite size effects in the short direction of the molecules, as witnessed by the results obtained for hydrogen-saturated nanoribbons, which may show a zero or non-zero band gap depending on the ribbon width or edge shape. Indeed, for large values of n, $X_{4n+2}H_{2n+4}$ closely resembles 2-ZXNR nanoribbon structures.[28] First-principles calculations on the latter give a direct gap 0.25 eV wide for X = Si[29] and ∼0.2 eV wide for X = C (*grafene*).[42] The above absolute values should be

https://dx.doi.org/10.1021/acsomega.0c01516
ACS Omega XXXX, XXX, XXX−XXX

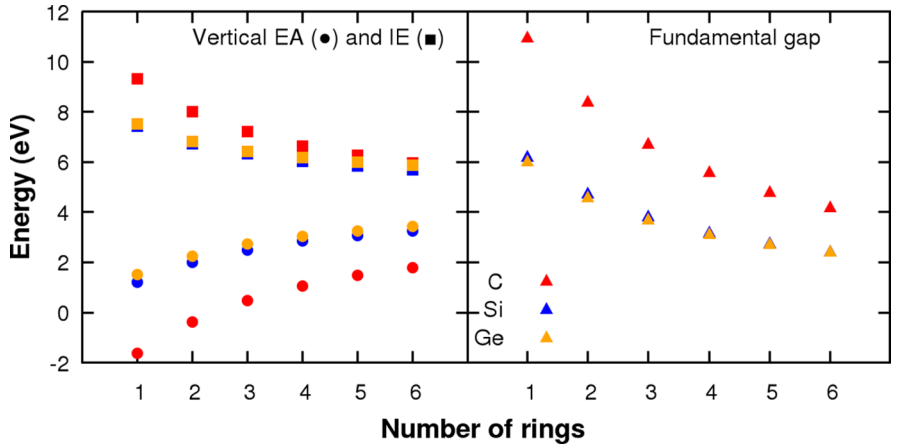

Figure 5. Computed electronic properties as a function of size. Vertical electron affiniy (EA_v) and vertical ionization energy (IE_v) are reported in the left panel, while the fundamental gap E_{gap} is shown in the right panel. Adopted color codes are red, blue, and orange for poly-C,Si,Ge-acenes, respectively.

Table 6. Energies (eV) of the p, α, and β Peaks as a Function of Molecular Size as Obtained Via TD-DFT Calculations for the Poly-C,Si,Ge-acenes Considered $X_{4n+2}H_{2n+4}$, with n = 1, 2, 3, 4, 5, 6[a]

n	p	α	β	E_{bind}
$C_{4n+2}H_{2n+4}$				
1	5.50/4.73[b] (<0.01)	6.22/5.96[b] (<0.001)	7.19/6.64[b] (1.20)	4.75
2	4.44/4.38[b] (0.06)	4.52/4.03[b] (<0.001)	6.01/5.62[b] (1.27)	3.96 (−17%)
3	3.27/3.38[b] (0.06)	3.91/3.57[b] (<0.001)	5.25/4.86[b] (1.98)	3.47 (−27%)
4	2.49/2.71[b] (0.05)	3.52/3.32[b] (0.001)	4.72/4.52[b] (2.68)	3.12 (−34%)
5	1.93/2.23[b] (0.04)	3.26/3.05[b] (0.004)	4.32/4.14[b] (3.34)	2.87 (−40%)
6	1.53/1.90[b] (0.03)	3.07/2.80[b] (0.009)	4.01 (3.95)	2.65 (−44%)
$Si_{4n+2}H_{2n+4}$				
1	2.84 (0.02)	2.46 (<0.001)	3.39 (0.69)	3.36
2	1.93 (0.04)	1.98/1.84[a] (<0.001/<0.001[a])	2.78/2.62[a] (0.76/0.62[a])	2.81 (−16%)
3	1.39 (0.03)	1.71 (<0.001)	2.41 (1.27)	2.42 (−28%)
4	1.04 (0.02)	1.54 (<0.001)	2.16 (1.83)	2.16 (−36%)
5	0.81 (0.02)	1.43 (0.001)	1.98 (2.41)	1.95 (−42%)
6	0.64 (0.02)	1.35/1.19[a] (0.003/0.006[a])	1.85/1.60[a] (2.98/1.44[a])	1.80 (−46%)
$Ge_{4n+2}H_{2n+4}$				
1	2.66 (0.03)	2.28 (<0.001)	3.17 (0.55)	3.34
2	1.83 (0.04)	1.87 (<0.001)	2.57 (0.58)	2.76 (−17%)
3	1.34 (0.03)	1.63 (0.001)	2.24 (0.97)	2.37 (−29%)
4	1.03 (0.03)	1.49 (0.006)	2.02 (1.41)	2.11 (−37%)
5	0.82 (0.02)	1.39 (0.017)	1.87 (1.86)	1.92 (−43%)
6	0.67 (0.02)	1.33 (0.035)	1.75 (2.34)	1.77 (−47%)

[a]The corresponding oscillator strengths are reported within parentheses. The last column reports the exciton binding energies E_{bind} with percentage deviation with respect to corresponding value of the smallest member in each class. All results have been obtained using B3PW91/TZVP, except for those marked with [a] achieved with BP86/TZVP and with [b]which are experimental values.[47]

taken only as estimates due to the well-known gap underestimation problem.[42] Interestingly, other works on 2-ZGNR[28] predict a zero gap.

OPTICAL PROPERTIES

Following the notation adopted for poly-C-acenes,[12,15] in Table 6, we report the main peak energy and oscillator strength of the so-called p, α, and β bands. The β and p bands correspond to the main peak and the optical onset of the absorption spectrum, respectively. The α band, on the contrary, is characterized by a negligile oscillator strength, which makes this transition usually non-detectable in the absorption spectrum.

The last column of Table 6 reports the exciton binding energy E_{bind} estimated as the difference between the fundamental gap E_{gap} and the optical gap E_{opt}, which corresponds to the p band energy. As expected, a general reduction of E_{bind} is observed in all cases as a consequence of a general decrease of confinement effects and reduction of screening as the molecular size increases.[44] Interestingly, while the relative reduction is roughly preserved along the three families (in the range from −20 to −50%), the values for poly-Si,Ge-acenes are almost coincident and on average smaller by about 30% with respect to the corresponding value for poly-C-acenes. The above results show that, at a fixed molecular size, poly-Si,Ge-acenes support less bounded excitons with respect to poly-C-acenes. This can be ascribed to the different interplay between the two ingredients entering E_{bind}, i.e., E_{gap} (which is larger for poly-C-acenes) and the optical onset (the energy of the p band) for C-acenes on one side and poly-Si,Ge-acenes on the other.

https://dx.doi.org/10.1021/acsomega.0c01516
ACS Omega XXXX, XXX, XXX−XXX

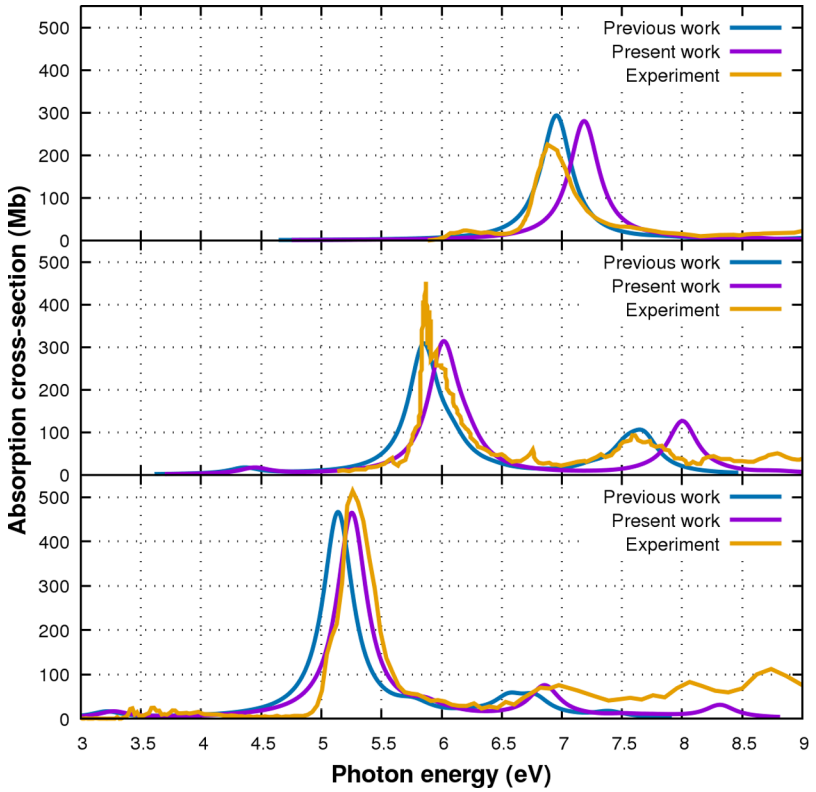

Figure 6. Comparison between the computed absorption cross section (Mb) and the previously published theoretical (ref 12) and experimental data (compiled in ref 14) for poly-C-acenes C, n = 1, 2, 3, from top to bottom, respectively.

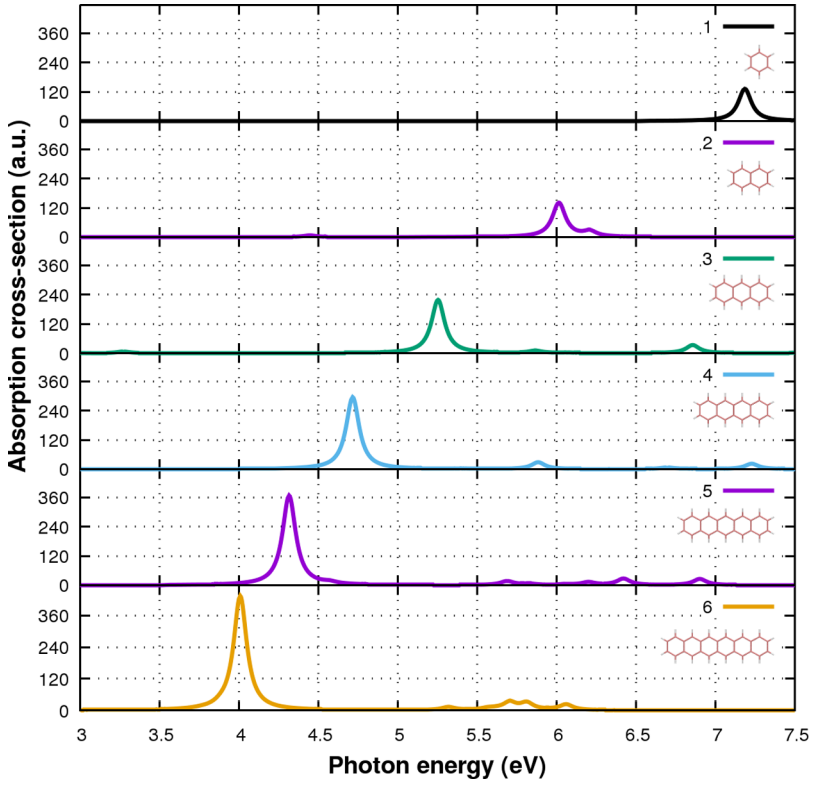

Figure 7. Absorption cross section (a.u.) for poly-C-acenes $C_{4n+2}H_{2n+4}$, n = 1, 2, 3, 4, 5, 6, from top to bottom, respectively.

In previous works on polyacenes,[12,15,45] it has been found that both β and α peaks correspond to transitions polarized along the main molecular axis, while the p band is polarized along the perpendicular direction. Such a behavior for p, α, and β is confirmed here, not only for C but also for Si and Ge (transition dipole moment data are not shown, but are available in the

https://dx.doi.org/10.1021/acsomega.0c01516
ACS Omega XXXX, XXX, XXX−XXX

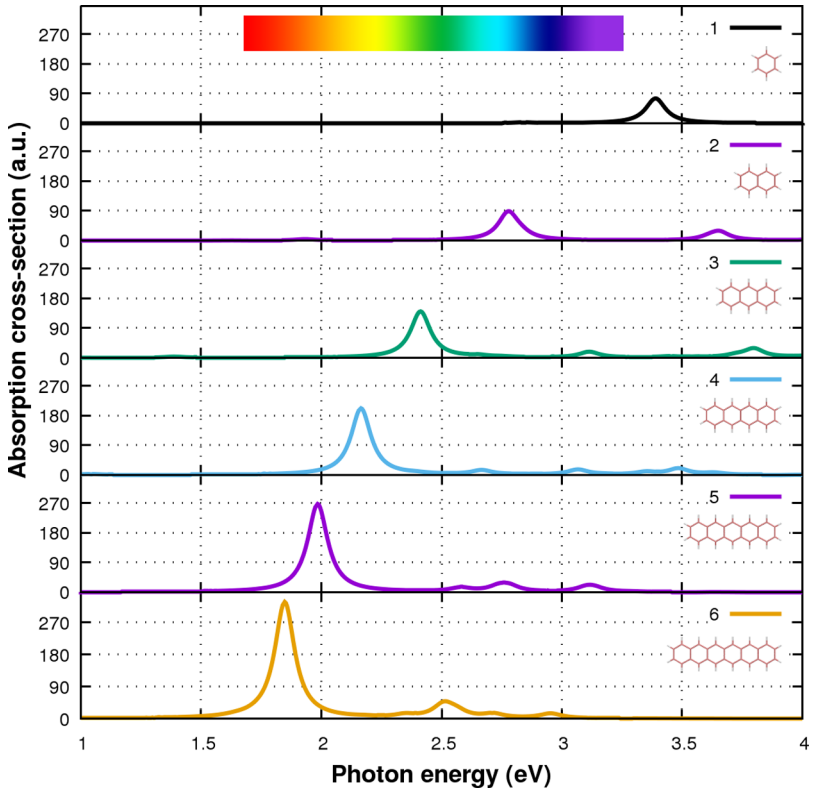

Figure 8. Absorption cross section (a.u.) for poly-Si-acenes $Si_{4n+2}H_{2n+4}$, n = 1, 2, 3, 4, 5, 6. The visible range is highlighted.

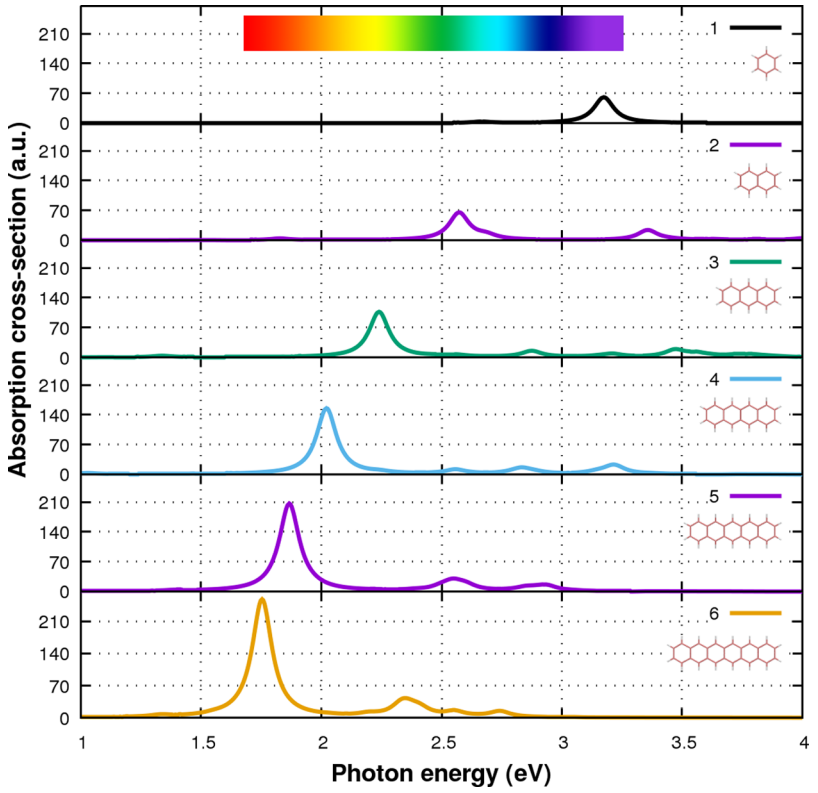

Figure 9. Absorption cross section (a.u.) for poly-Ge-acenes $Ge_{4n+2}H_{2n+4}$, n = 1, 2, 3, 4, 5, 6. The visible range is highlighted.

Supporting Information of ref 46). The data reported for p, α, and β bands of poly-C-acenes agree with those previously obtained at a different level of theory (B3LYP/6-31 + G*),[12,14,15] and are in fairly good agreement with the available experimental data[18] (marked with b in Table 6). As an example, Figure 6 compares the absorption spectra for the first three members of the poly-C-acenes class.

https://dx.doi.org/10.1021/acsomega.0c01516
ACS Omega XXXX, XXX, XXX−XXX

Comparison of the results for poly-Si-acenes with ref 48 reveals that our α and β peaks are located at energies ~0.25 eV higher, as expected due to the different exchange-correlation functional adopted (BP86 in ref 48, B3PW91 in the present work). We indeed verified for $Si_{10}H_8$ and $Si_{26}H_{16}$ that TD-DFT calculations at the BP86/TZVP level of theory (marked with a in Table 6) make our data virtually coincident, within numerical errors, with those of ref 48.

As expected, and consistently with previous findings, we found in all cases that the energy of the main transitions decreases as a function of molecular size, while the corresponding oscillator strength increases. This is clearly seen in Figures 7−9, displaying the absorption spectra up to the near-UV of all the species considered. Inspection of the above figures confirms visually the main trend previously observed for all families: a general red shift of the optical onsets and the dominant peaks as a function of the molecular dimension. In addition, for C-acenes, the strongest β transition always has B_{2u} symmetry, while the symmetry of the most important higher energy peaks (oscillator strength greater than 0.1) changes from B_{1u} (polarization perpendicular to the long axis) to B_{2u} (polarization aligned with long axis) when n increases from 2 to 6. Similarly, Si- and Ge-acenes show A_u symmetry for the strongest β peaks, and we observe a shift from B_u (polarization perpendicular to the long axis) to A_u (polarization aligned with long axis) for the higher energy transitions when the size of the molecule increases. The complete sets of 50 electronic transitions, computed at the TD-DFT level, for all poly-C,Si,Ge-acenes with n = 2, 3, 4, 5, 6, are available in the Supporting Information of ref 46.

In particular, it is instructive to compare the positions of the strongest features in the absorption spectra for the three families considered. Figure 10 displays, as a function of molecular size,

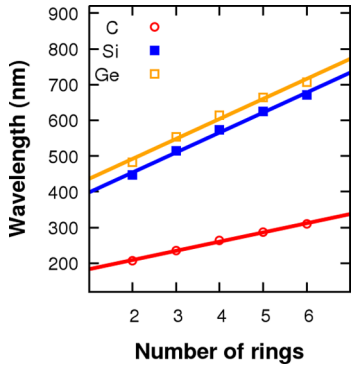

Figure 10. β peak excitation wavelengths (nm) of poly-C,Si,Ge-acenes from two to six rings. A linear relationship between the wavelengths of the β peak and the cluster size (number of rings) can be observed.

the wavelength of the β peaks (expressed in nm) and the straight line fitting the data for the poly-C,Si,Ge-acenes considered. Interestingly, poly-Si,Ge-acenes display similar slopes, ~56 nm, although the peak positions of the former are located at lower wavelengths. Other authors[48] find a value of ~77 nm for Si, but the difference can be ascribed to the different levels of theory as discussed before. On the other hand, the β peak positions of poly-C-acenes fall at much shorter wavelengths and appear to be distributed along a straight line with considerably lower slope, ~26 nm, in good agreement with experimental data[47] and previous theoretical results.[49]

The main absorption peaks for C-acenes fall in the UV part of the spectrum, while for poly-Si,Ge-acenes, this is true only for the smallest cluster. As observed elsewhere[48] for both poly-Si,Ge-acenes, the excitation energies of the β peaks span the visible region of the spectrum, and this demonstrates the tunability of these systems as a function of size. In addition, as already shown for polyacenes[49,50] and poly-Si-acenes,[8] we find in all cases that the same transitions contribute to α and β peaks (e.g. HOMO → LUMO+1 and HOMO-1 → LUMO for $X_{10}H_8$ and $X_{14}H_{10}$, X = C,Si,Ge). While in the former case, the addition of transition dipole moments is destructive (similar amplitudes but with opposite signs); in the latter case it is constructive, and this results in low and high oscillator strengths, respectively. This is recognized[8,49] as the signature of the plasmonic origin of the β peaks. It is interesting to notice that destructive interaction for α peaks decreases (i.e., strength increases) with size.

CONCLUSIONS

We presented a systematic (TD)-DFT study of the morphological, electronic, and optical properties of poly-C,Si,Ge-acenes ($X_{4n+2}H_{2n+4}$, X = C,Si,Ge, n = 1, 2, 3, 4, 5, 6). We compared our results with existing theoretical data for 2D lattices and nanoribbons and available experiments. Analysis of the morphological properties confirms previous results; according to which, while C-based acenes are planar, both Si- and Ge-based counterparts assume a buckled configuration. Concerning electronic properties, we found for each family a general increase (decrease) of the vertical electron affinities (ionization energies) as a function of size. This gives rise to an overall closure of the fundamental electronic gap, as expected from quantum confinement effects. Independently of the nature of the atomic constituents, this property is reflected in a general red shift of both the optical onset and the position of the dominant UV−visible absorption peaks, as a function of size. In particular, we found a linear relationship describing the wavelength-dependence of the β peaks with the number of rings and a similar slope of about 56 nm is observed for Si- and Ge-acenes. The present investigation contributes to the search of new, complementary materials for opto-electronic applications and devices.

COMPUTATIONAL METHODS

Ground-state electronic properties were computed in the framework of the density functional theory.[51] Following previous studies on poly-Si-acenes,[9,48,52] geometry optimizations were performed using the B3PW91 hybrid exchange-correlation functional,[53,54] combined with the TZVP basis-set, a triple-ζ valence basis set with one set of polarization d-functions on heavy atoms and one set of p-functions on hydrogen atoms.[55] We computed vertical electron affinities (EA_v) and ionization energies (IE_v) via total energy differences by considering the ±1 charged species at the neutral optimized geometry. According to the ΔSCF method[56,57] the fundamental gap is given by

$$E_{gap} = IE_v - EA_v = (E_{N-1} - E_N) - (E_N - E_{N+1}) \quad (1)$$

E_M, $(M = N - 1, N, N + 1)$ being the total energy of the M-electron system. To obtain the electronic absorption spectra, we performed time-dependent DFT (TD-DFT)[58] calculations at the same level of theory B3PW91/TZVP employed for ground-state calculations. We used the frequency space implementation in which the poles of the linear response function correspond to vertical excitation energies and pole strengths represent oscillator strengths.[59] TD-DFT is an efficient and powerful

https://dx.doi.org/10.1021/acsomega.0c01516
ACS Omega XXXX, XXX, XXX−XXX

scheme for the calculation of the absorption spectra of finite systems, typically yielding results in very good agreement with available experimental data.[15,60,61] The many-body perturbation theory can be used to compute optical absorption spectra of molecules and clusters.[62,63] However, while this technique has proven to provide results in very good agreement with high-level quantum chemistry techniques,[64] it is computationally intensive and not suited for a systematic comparative investigation like the one presented here. We estimate exciton-binding energies (E_{bind}) by subtracting the energy of the first optically active transition (E_{opt}) from that of the fundamental gap (E_{gap}): $E_{bind} = E_{gap} - E_{opt}$.[57,62,65] E_{bind} is one of the key parameters regulating the optical absorption of materials.[44] All calculations were performed using the Gaussian-09 software package,[66] and images were rendered with the VMD software.[67] Input and output Gaussian files, as well as the list of 50 computed electronic transitions for each molecule are freely available at https://www.dsf.unica.it/csige.

AUTHOR INFORMATION

Corresponding Authors

Giuliano Malloci − *Department of Physics, University of Cagliari, I-09042 Monserrato, CA, Italy;* orcid.org/0000-0002-5985-257X; Email: giuliano.malloci@dsf.unica.it

Giancarlo Cappellini − *Department of Physics, University of Cagliari, I-09042 Monserrato, CA, Italy;* orcid.org/0000-0001-9746-3025; Email: giancarlo.cappellini@dsf.unica.it

Authors

Paola Mocci − *Department of Physics, University of Cagliari, I-09042 Monserrato, CA, Italy*

Andrea Bosin − *Department of Physics, University of Cagliari, I-09042 Monserrato, CA, Italy;* orcid.org/0000-0001-6300-5712

Complete contact information is available at: https://pubs.acs.org/10.1021/acsomega.0c01516

Notes

The authors declare no competing financial interest.

ACKNOWLEDGMENTS

G.C. acknowledges partial financial support from IDEA-AISBL Bruxelles. P.M. acknowledges the PhD school of the University of Cagliari. All the authors acknowledge helpful discussions with R. Cardia and G. Serra.

REFERENCES

(1) Geim, A. K. Nobel Lecture: Random walk to graphene. *Rev. Mod. Phys.* **2011**, *83*, 851−862.

(2) Mas-Ballesté, R.; Gómez-Navarro, C.; Gómez-Herrero, J.; Zamora, F. 2D materials: to graphene and beyond. *Nanoscale* **2011**, *3*, 20−30.

(3) John, R.; Merlin, B. Optical properties of graphene, silicene, germanene, and stanene, from IR to far UV − A first principles study. *J. Phys. Chem. Solids* **2017**, *110*, 307−315.

(4) Ni, Z.; Liu, Q.; Tang, K.; Zheng, J.; Zhou, J.; Qin, R.; Gao, Z.; Yu, D.; Lu, J. Tunable Bandgap in Silicene and Germanene. *Nano Lett.* **2011**, *12*, 113−118.

(5) Acun, A.; Zhang, L.; Bampoulis, P.; Farmanbar, M.; van Houselt, A.; Rudenko, A. N.; Lingenfelder, M.; Brocks, G.; Poelsema, B.; Katsnelson, M. I.; Zandvliet, H. J. W. Germanene: the germanium analogue of graphene. *J. Phys.: Condens. Matter* **2015**, *27*, 443002.

(6) Matthes, L.; Gori, P.; Pulci, O.; Bechstedt, F. Universal infrared absorbance of twodimensional honeycomb group-IV crystals. *Phys. Rev. B* **2013**, *87*, No. 035438.

(7) Dávila, M. E.; Xian, L.; Cahangirov, S.; Rubio, A.; Le Lay, G. Germanene: a novel two-dimensional germanium allotrope akin to graphene and silicene. *New J. Phys.* **2014**, *16*, No. 095002.

(8) Jose, D.; Datta, A. Structures and electronic properties of silicene clusters: a promising material for FET and hydrogen storage. *Phys. Chem. Chem. Phys.* **2011**, *13*, 7304−7311.

(9) Mokkath, J. H.; Schwingenschlögl, U. Tunable optical absorption in silicene molecules. *J. Mater. Chem. C* **2016**, *4*, 7387−7390.

(10) Bechstedt, F.; Matthes, L.; Gori, P.; Pulci, O. Infrared absorbance of silicene and germanene. *Appl. Phys. Lett.* **2012**, *100*, 261906.

(11) Özçelik, V. O.; Kecik, D.; Durgun, E.; Ciraci, S. Adsorption of Group IV Elements on Graphene, Silicene, Germanene, and Stanene: Dumbbell Formation. *J. Phys. Chem. C* **2014**, *119*, 845−853.

(12) Malloci, G.; Mulas, G.; Cappellini, G.; Joblin, C. Time-dependent density functional study of the electronic spectra of oligoacenes in the charge states −1, 0, +1, and +2. *Chem. Phys.* **2007**, *340*, 43−58.

(13) Malloci, G.; Joblin, C.; Mulas, G. On-line database of the spectral properties of polycyclic aromatic hydrocarbons. *Chem. Phys.* **2007**, *332*, 353−359.

(14) Cappellini, G.; Malloci, G.; Mulas, G. Electronic excitations of oligoacenes: A time dependent density functional theory study. *Superlattices Microstruct.* **2009**, *46*, 14−18.

(15) Malloci, G.; Cappellini, G.; Mulas, G.; Mattoni, A. Electronic and optical properties of families of polycyclic aromatic hydrocarbons: A systematic (time-dependent) density functional theory study. *Chem. Phys.* **2011**, *384*, 19−27.

(16) Du, C.; Guo, Y.; Chen, J.; Liu, H.; Liu, Y.; Ye, S.; Lu, K.; Zheng, J.; Wu, T.; Liu, Y.; Shuai, Z.; Yu, G. Design, Synthesis, and Properties of Asymmetrical Heteroacene and Its Application in Organic Electronics. *J. Phys. Chem. C* **2010**, *114*, 10565−10571.

(17) Figueira-Duarte, T. M.; Müllen, K. Pyrene-Based Materials for Organic Electronics. *Chem. Rev.* **2011**, *111*, 7260−7314.

(18) Anthony, J. E. Addressing challenges. *Nat. Mater.* **2014**, *13*, 773−775.

(19) Cardia, R.; Malloci, G.; Mattoni, A.; Cappellini, G. Effects of TIPS-Functionalization and Perhalogenation on the Electronic, Optical, and Transport Properties of Angular and Compact Dibenzochrysene. *J. Phys. Chem. A* **2014**, *118*, 5170−5177.

(20) Cardia, R.; Malloci, G.; Rignanese, G.-M.; Blase, X.; Molteni, E.; Cappellini, G. Electronic and optical properties of hexathiapentacene in the gas and crystal phases. *Phys. Rev. B* **2016**, *93*, 235132.

(21) Aumaitre, C.; Morin, J.-F. Polycyclic Aromatic Hydrocarbons as Potential Building Blocks for Organic Solar Cells. *Chem. Rec.* **2019**, *19*, 1142−1154.

(22) Dewar, M. J. S.; Lo, D. H.; Ramsden, C. A. Ground states of molecules. XXIX. MINDO/3 calculations of compounds containing third row elements. *J. Am. Chem. Soc.* **1975**, *97*, 1311−1318.

(23) Nagase, S.; Teramae, H.; Kudo, T. Hexasilabenzene (Si_6H_6). Is the benzene-like D_{6h} structure stable? *J. Chem. Phys.* **1987**, *86*, 4513−4517.

(24) Ivanov, A. S.; Boldyrev, A. I. $Si_{6-n}C_nH_6$ (n = 0−6) Series: When Do Silabenzenes Become Planar and Global Minima? *J. Phys. Chem. A* **2012**, *116*, 9591−9598.

(25) Jose, D.; Datta, A. Understanding of the Buckling Distortions in Silicene. *J. Phys. Chem. C* **2012**, *116*, 24639−24648.

(26) Jose, D.; Datta, A. Structures and Chemical Properties of Silicene: Unlike Graphene. *Acc. Chem. Res.* **2014**, *47*, 593−602.

(27) Nijamudheen, A.; Bhattacharjee, R.; Choudhury, S.; Datta, A. Electronic and Chemical Properties of Germanene: The Crucial Role of Buckling. *J. Phys. Chem. C* **2015**, *119*, 3802−3809.

(28) Miyamoto, Y.; Nakada, K.; Fujita, M. First-principles study of edge states of H-terminated graphitic ribbons. *Phys. Rev. B* **1999**, *59*, 9858−9861.

(29) Song, Y.-L.; Zhang, Y.; Zhang, J.-M.; Lu, D.-B. Effects of the edge shape and the width on the structural and electronic properties of silicene nanoribbons. *Appl. Surf. Sci.* **2010**, *256*, 6313−6317.

https://dx.doi.org/10.1021/acsomega.0c01516
ACS Omega XXXX, XXX, XXX−XXX

(30) Cahangirov, S.; Topsakal, M.; Ciraci, S. Armchair nanoribbons of silicon and germanium honeycomb structures. *Phys. Rev. B* **2010**, *81*, 195120.
(31) Liu, J.; Yu, G.; Shen, X.; Zhang, H.; Li, H.; Huang, X.; Chen, W. The structures, stabilities, electronic and magnetic properties of fully and partially hydrogenated germanene nanoribbons: A first-principles investigation. *Phys. E* **2017**, *87*, 27−36.
(32) Pablo-Pedro, R.; Lopez-Rios, H.; Mendoza-Cortes, J.-L.; Kong, J.; Fomine, S.; Van Voorhis, T.; Dresselhaus, M. S. Exploring Low Internal Reorganization Energies for Silicene Nanoclusters. *Phys. Rev. Appl.* **2018**, *9*, No. 054012.
(33) Shiraz, A. K.; Goharrizi, A. Y.; Hamidi, S. M. The electronic and optical properties of armchair germanene nanoribbons. *Phys. E* **2019**, *107*, 150−153.
(34) Ferri, M.; Fratesi, G.; Onida, G.; Debernardi, A. Ab initio study of the structural, electronic, magnetic, and optical properties of silicene nanoribbons. *Phys. Rev. B* **2019**, *99*, No. 085414.
(35) Wakita, K.; Tokitoh, N.; Okazaki, R.; Takagi, N.; Nagase, S. Crystal Structure of a Stable Silabenzene and Its Photochemical Valence Isomerization into the Corresponding Silabenzvalene. *J. Am. Chem. Soc.* **2000**, *122*, 5648−5649.
(36) Takeda, N.; Shinohara, A.; Tokitoh, N. Synthesis and Properties of the First 1-Silanaphthalene. *Organometallics* **2002**, *21*, 4024−4026.
(37) Wakita, K.; Tokitoh, N.; Okazaki, R.; Nagase, S.; von Ragué Schleyer, P.; Jiao, H. Synthesis of Stable 2-Silanaphthalenes and Their Aromaticity. *J. Am. Chem. Soc.* **1999**, *121*, 11336−11344.
(38) Takeda, N.; Shinohara, A.; Tokitoh, N. The First Stable 9-Silaanthracene. *Organometallics* **2002**, *21*, 256−258.
(39) Abersfelder, K.; White, A. J. P.; Rzepa, H. S.; Scheschkewitz, D. A Tricyclic Aromatic Isomer of Hexasilabenzene. *Science* **2010**, *327*, 564−566.
(40) Deng, Z.; Li, Z.; Wang, W. Electron affinity and ionization potential of two-dimensional honeycomb sheets: A first principle study. *Chem. Phys. Lett.* **2015**, *637*, 26−31.
(41) Kittel, C. *Introduction to Solid State Physics*; 8th ed.; John Wiley and Sons: 2005.
(42) Son, Y.-W.; Cohen, M. L.; Louie, S. G. Energy Gaps in Graphene Nanoribbons. *Phys. Rev. Lett.* **2006**, *97*, 216803.
(43) Hajgató, B.; Deleuze, M. S.; Tozer, D. J.; De Proft, F. A benchmark theoretical study of the electron affinities of benzene and linear acenes. *J. Chem. Phys.* **2008**, *129*, No. 084308.
(44) Knupfer, M. Exciton binding energies in organic semiconductors. *Appl. Phys. A* **2003**, *77*, 623−626.
(45) Sony, P.; Shukla, A. Large-scale correlated calculations of linear optical absorption and low-lying excited states of polyacenes: Pariser-Parr-Pople Hamiltonian. *Phys. Rev. B* **2007**, *75*, 155208.
(46) Supporting material. https://www.dsf.unica.it/csige.
(47) Biermann, D.; Schmidt, W. Diels-Alder reactivity of polycyclic aromatic hydrocarbons. 1. Acenes and benzologs. *J. Am. Chem. Soc.* **1980**, *102*, 3163−3173.
(48) Weerawardene, K. L. D. M.; Aikens, C. M. Strong Tunable Visible Absorption Predicted for Polysilo-acenes Using TDDFT Calculations. *J. Phys. Chem. Lett.* **2015**, *6*, 3341−3345.
(49) Guidez, E. B.; Aikens, C. M. Origin and TDDFT Benchmarking of the Plasmon Resonance in Acenes. *J. Phys. Chem. C* **2013**, *117*, 21466−21475.
(50) Guidez, E. B.; Aikens, C. M. Quantum mechanical origin of the plasmon: from molecular systems to nanoparticles. *Nanoscale* **2014**, *6*, 11512−11527.
(51) Kohn, W. Nobel Lecture: Electronic structure of matter—wave functions and density functionals. *Rev. Mod. Phys.* **1999**, *71*, 1253−1266.
(52) Echegoyen, L.; Echegoyen, L. E. Electrochemistry of Fullerenes and Their Derivatives. *Acc. Chem. Res.* **1998**, *31*, 593−601.
(53) Becke, A. D. Density-functional thermochemistry. III. The role of exact exchange. *J. Chem. Phys.* **1993**, *98*, 5648−5652.
(54) Lee, C.; Yang, W.; Parr, R. G. Development of the Colle-Salvetti correlation-energy formula into a functional of the electron density. *Phys. Rev. B* **1988**, *37*, 785−789.
(55) Schäfer, A.; Horn, H.; Ahlrichs, R. Fully optimized contracted Gaussian basis sets for atoms Li to Kr. *J. Chem. Phys.* **1992**, *97*, 2571−2577.
(56) Jones, R. O.; Gunnarsson, O. The density functional formalism, its applications and prospects. *Rev. Mod. Phys.* **1989**, *61*, 689−746.
(57) Malloci, G.; Cappellini, G.; Mulas, G.; Satta, G. Quasiparticle effects and optical absorption in small fullerenelike GaP clusters. *Phys. Rev. B* **2004**, *70*, 205429.
(58) Runge, E.; Gross, E. K. U. Density-Functional Theory for Time-Dependent Systems. *Phys. Rev. Lett.* **1984**, *52*, 997−1000.
(59) Casida, M. E. Time-Dependent Density Functional Response Theory for Molecules. In *Recent Advances in Density Functional Methods*; World Scientific: 1995, *1*, 155−192.
(60) Sancho-García, J. C. Assessment of density-functional models for organic molecular semiconductors: The role of Hartree−Fock exchange in charge-transfer processes. *Chem. Phys.* **2007**, *331*, 321−331.
(61) Malloci, G.; Chiodo, L.; Rubio, A.; Mattoni, A. Structural and Optoelectronic Properties of Unsaturated ZnO and ZnS Nanoclusters. *J. Phys. Chem. C* **2012**, *116*, 8741−8746.
(62) Dardenne, N.; Cardia, R.; Li, J.; Malloci, G.; Cappellini, G.; Blase, X.; Charlier, J.-C.; Rignanese, G.-M. Tuning Optical Properties of Dibenzochrysenes by Functionalization: A Many-Body Perturbation Theory Study. *J. Phys. Chem. C* **2017**, *121*, 24480−24488.
(63) Cazzaniga, M.; Cargnoni, F.; Penconi, M.; Bossi, A.; Ceresoli, D. Ab Initio ManyBody Perturbation Theory Calculations of the Electronic and Optical Properties of Cyclometalated Ir(III) Complexes. *J. Chem. Theory Comput.* **2020**, *16*, 1188−1199.
(64) Jacquemin, D.; Duchemin, I.; Blase, X. Benchmarking the Bethe−Salpeter Formalism on a Standard Organic Molecular Set. *J. Chem. Theory Comput.* **2015**, *11*, 3290−3304.
(65) Malloci, G.; Cappellini, G.; Mulas, G.; Mattoni, A. A (time-dependent) density functional theory study of the optoelectronic properties of bis-triisopropylsilylethynyl-functionalized acenes. *Thin Solid Films* **2013**, *543*, 32−34.
(66) Frisch, M. J.; et al. *Gaussian09 Revision A.02*; Gaussian Inc.: Wallingford CT, 2009.
(67) Humphrey, W.; Dalke, A.; Schulten, K. VMD − Visual Molecular Dynamics. *J. Mol. Graphics* **1996**, *14*, 33−38.

https://dx.doi.org/10.1021/acsomega.0c01516
ACS Omega XXXX, XXX, XXX−XXX